

cal jitter analysis, and thus it is used in the following experiments.

3. Jitter performance and amplitude stability of clock recovery for degraded input signals

First we analyzed the retiming function of the optical clock by use of the experimental setup depicted in Figure 1. A 40 Gb/s true PRBS 2^{7-1} data stream generated by gain-switched-laser (GSL) is launched into the PhaseCOMB-laser. Figure 3a shows the eye diagram of the non-intentionally degraded data signal (upper trace) and the recovered clock (lower trace). The rms-jitter of the data signal amounts to 1100 fs. The rms jitter of the extracted clock signal is 510 fs which is significantly less than the jitter of the data signal. Now the data signal was strongly degraded by

additional timing jitter (Fig. 3b upper trace). Note the time stability of the clock signal is preserved. Even for a data input signal with a very high jitter of 2000 fs the jitter of the recovered clock remains well below 600 fs. Fig. 3c summarizes the non linear relation between clock output jitter and data input jitter. One can see there is always an improvement towards lower jitter values by applied optical clock recovery. Thus the excellent retiming function of the PhaseCOMB-laser is verified.

Next we investigated the performance of the PhaseCOMB-laser versus amplitude fluctuations of the data signal. The power level of the PRBS signal was decreased from +6 dBm down to +2 dBm as shown in Figure 4a (upper trace). For this

measurement we used the average function of the sampling scope. It can be observed, the sinusoidal pulse trace of the clock remains stable in amplitude and in time (Fig. 4a lower trace) although the eye opening of the data signal is nearly closed. The large dynamic range of the optical clock becomes clearly evident in Figure 4b. The rms-jitter of the clock recovery keeps nearly constant (below 600 fs) while the locking power level changes in the range from 0 dBm to +8 dBm.

4. Locking range of the optical clock

For system application a wide locking range is preferable. Figure 5 shows the two rf-spectra edges of the unlocked PhaseCOMB-laser and the matched sharp rf-line of the synchronized clock locked to 39.813 Gb/s RZ data signals with 8 dBm optical power. Within a frequency range of 250 MHz the rms-jitter remains constant and is below 600 fs - while jitter increases beyond. Thus the clock can be operated error free in 40 Gb/s systems within a 250 MHz locking range which is much larger than that of the electronic PLL (~ kHz).

5. Conclusions

We reported on jitter analysis of PhaseCOMB-lasers at 40 GHz using a sampling scope with novel precision time base reference module. The magnificent reduction of jitter by the recovered clock was demonstrated even for strongly degraded signals. The large dynamic range (8 dBm) preserving constant rms-jitter below 600 fs as well as the wide locking range of 250 MHz predict this semiconductor device to be very promising for application in high speed optical signal processing systems.

6. References

1. C. Bornholdt et al., "Self-pulsating DFB-laser for all-optical clock recovery at 40 Gb/s." *Electron. Lett.* 36, pp. 327-328, 2000.
2. C. Bornholdt et al., "Application of a 80 GHz all-optical clock in a 160 km transmission experiment." TuN6 OFC 2002, Anaheim, California.
3. H. J. Wünsche, H. P. Nolting et al., "Modelling of devices for all-optical 3R-regeneration." IWA1 (invited), IPR 2001, Monterey, California.
4. B. Sartorius et al., "All-optical clock recovery for signal processing and regeneration." TuB3 (invited), IEEE/ LEOS 2002, Summer Topical Meeting, Mont Tremblant, QC Canada.

MF98

5:30 PM

Polarization Insensitive Waveform Restoration and Channel Crosstalk Reduction in Semiconductor Optical Amplifier Gates Using Polarimetric Filtering

K. Chan, C. K Chan, L. K. Chen, F. Tong, *Department of Information Engineering, The Chinese University of Hong Kong, Shatin, N.T., Hong Kong Special Administrative Region of China, Email: kchan0@ie.cuhk.edu.hk.*

We present a polarization-insensitive approach for waveform restoration in semiconductor-optical-amplifier (SOA) based optical gates using nonlinear polarization rotation in SOA and polarimetric filtering. The scheme is capable of suppressing the channel crosstalk owing to SOA's cross-gain-modulation for multiple input wavelengths.

1. INTRODUCTION

The semiconductor optical amplifier (SOA) has recently attracted much attention because of its wide applications, not only for in-line optical amplification, but also for gating control in optical cross-connects and packet switching networks. The application of SOA gates is advantageous because of its optical gain and fast response. To ensure a good optical signal-to-noise ratio (OSNR), it is preferable to operate the SOA gates in gain saturation regime. However, its fast gain dynamics causes pattern dependent distortion which severely distorts the output signal waveform. Several solutions were proposed, including gain clamping [1], shifting the output wavelength [2] and light injection [3-4]. Yet these schemes had their own limitations in terms of complexity, gain consumption and signal bit rate. In [5], waveform restoration based on nonlinear polar-

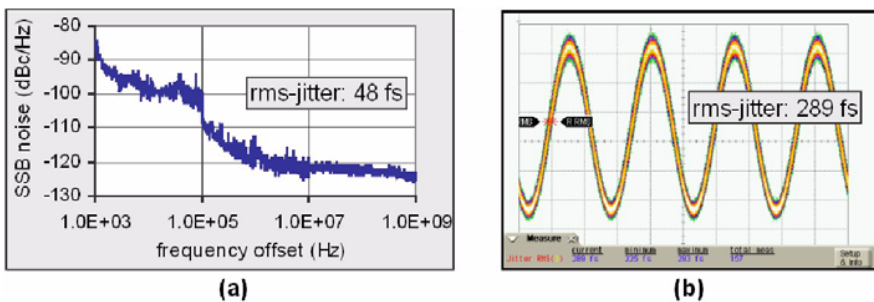


Fig. 2. Jitter performance of optical clock for ideal input signal evaluated by (a) single sideband phase noise measurement with rf-analyzer and (b) by sampling scope including precision time base reference module

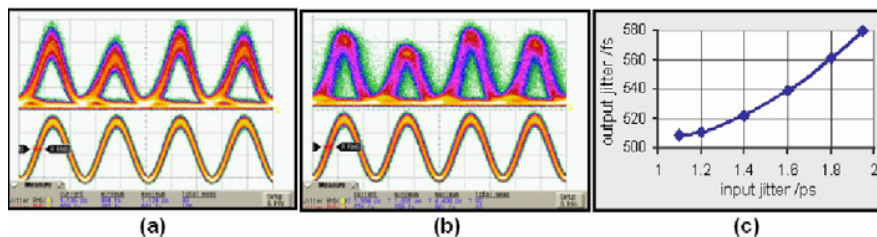


Fig. 3. 40Gb/s data signal (upper traces a, b), recovered clock (lower traces a, b) and input versus output jitter (c)

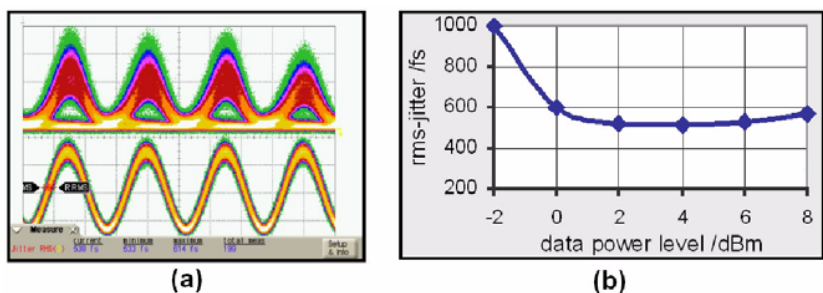


Fig. 4. Dynamic range of optical clock recovery

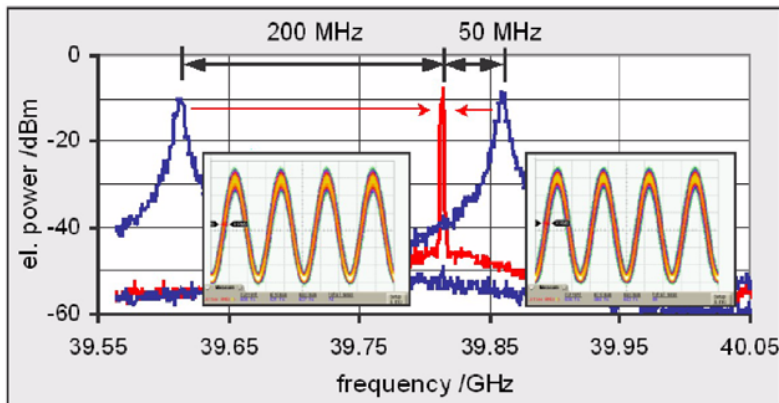


Fig. 5. Locking range of optical clock recovery

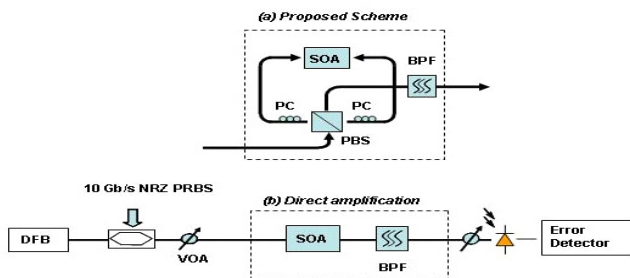


Figure 1 Experiment setup. VOA: variable optical attenuator; SOA: semiconductor optical amplifier; PBS: polarization beam splitter; PC: polarization controller; BPF: optical bandpass filter.

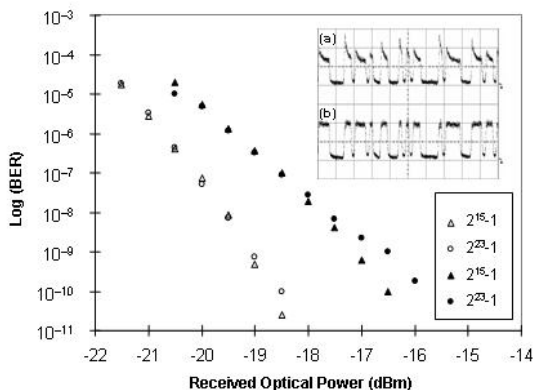


Figure 2 Bit error rate (BER) measurement of 10-Gb/s PRBS with lengths of $2^{15}-1$ and $2^{23}-1$. open symbols: proposed scheme; solid symbols: direct SOA amplification. Insets: pulse pattern with PRBS length of 2^7-1 for (a) direct amplification (b) proposed scheme

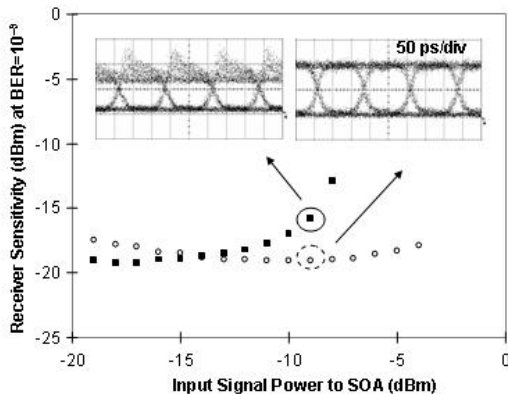


Figure 3 Receiver sensitivity at BER of 10^{-9} as a function of input signal power. 10-Gb/s PRBS sequence length = $2^{23}-1$. open symbols: proposed scheme; solid symbols: direct SOA amplification. Insets show the respective eye diagrams for input signal power is -11 dBm.

ization rotation in SOA was discussed. However, the performance was sensitive to the input signal polarization. In this paper, we demonstrate an effective and polarization insensitive scheme to achieve waveform restoration based on nonlinear polarization rotation in SOA. SOA gate operation with high input power dynamic range (IPDR) can be achieved and an output OSNR of above 35 dB is obtained with negligible waveform distortion. The proposed scheme can also effectively restore the distorted waveform caused by cross gain modulation (XGM) in multi-wavelength scenario.

2. SCHEME AND PRINCIPLE

For an SOA operating in saturation regime, the decrease in carrier density results in gain suppression. The leading edge of each input non-return-to-zero (NRZ) pulse experiences relatively much larger gain than the other part of the pulse, thus

intense spikes are resulted at the leading edges of the amplified signal. The output signal waveform is thus severely distorted. Concurrently, the gain suppression is accompanied by phase modulation of the signal. Because of the induced birefringence in SOA, the input signal polarization is rotated at the output of SOA in which a larger polarization rotation is obtained at the pulse's leading edges as compared to the other part of the pulses. Hence, by placing a polarizer at the output of SOA, the over-amplified spikes can be suppressed and thus the distorted waveform can be restored. In our proposed scheme, we utilize a polarization diversified fiber loop that splits and injects the input signal into the SOA from both sides to effectively alleviate the dependence of the input signal polarization. It is crucial that the SOA is placed at the mid-point of the fiber loop so as to

avoid the possible crosstalk induced by XGM in the SOA.

3. EXPERIMENT AND RESULT

The experimental setup is shown in Fig. 1. Light from the DFB laser was modulated by a LiNbO₃ modulator using a 10-Gbit/s NRZ PRBS data sequence. A variable optical attenuator (VOA) was used to control the transmitted optical power. The SOA was located at the center of the fiber loop. The input signal is split at the polarization beam splitter (PBS) and the two signals were launched into the SOA from both directions. At the output of the PBS, a 1-nm optical bandpass filter (OBPF) was used to filter out the amplified spontaneous emission (ASE) from the SOA. For comparison, a direct amplification experiment using SOA was also performed as shown in Fig. 1(b). Input power was recorded at the input of the SOA, such that the degree of gain saturation is the same in both cases.

Fig. 2 shows the corresponding BER performance in both cases. It is clearly shown that, for PRBS lengths of $2^{15}-1$ and $2^{23}-1$, more than 2-dB reduction in power penalty was achieved by using our proposed scheme. To illustrate the waveform restoration with PRBS length of 2^7-1 is also shown in the inset, where no significant pattern dependence was observed. The waveforms of the output pulse train were obtained from the SOA for (a) direct amplification case and (b) our proposed scheme using polarization diversified fiber loop at an optical input power of -11 dBm. Owing to gain saturation in SOA, it was found that in the former case, the leading edges of "1" bits experienced a much higher gain than the rest part of the optical pulses, while in the latter case, the waveform was much improved as the over-amplified leading edges of ones were eliminated by polarization filtering.

We also measured the SOA input power dynamic range (IPDR) for both cases by adjusting the VOA placed after the transmitter. The results were depicted in Fig. 3. The receiver sensitivity was obtained at a BER of 10^{-9} against different input signal powers. For the case of direct amplification, the rapid increase in the power penalty was attributed to the distorted waveform due to gain saturation in SOA. It was shown that our proposed scheme achieved a transmission window of about 13 dB at 1-dB power penalty. Comparing with the case of direct amplification, the proposed scheme has extended the input power dynamic range to the high power end by 8 dB. This implies high output OSNR could be obtained with much reduced waveform distortion.

To study the polarization sensitivity of our proposed scheme, a $\lambda/2$ wave plate was placed before the polarization diversified fiber loop. A variation of less than 0.4 dB in the receiver sensitivity at BER of 10^{-9} was observed by continuously rotating the $\lambda/2$ wave plate.

For SOA operated in saturation regime with multi-channel input, channel crosstalk is always a critical issue due to XGM in SOA. In our experiment, we also investigated the performance of our proposed scheme with multi-wavelength input. Two-channel input was tested with wavelengths centered at 1548 nm and 1553 nm respectively. The input optical power was also adjusted to be at -11 dBm. A similar experimental setup as shown in Fig. 1 was used except that the two input wavelengths, each modulated at 10-Gb/s, were first fed into a piece of 1-km dispersion compensation fiber (DCF) for channel decorrelation before being launched into the polarization diversified fiber loop. By appropriate setting the two polarization controllers in the two arms of the fiber loop, the XGM-induced crosstalk in both wavelength channels were observed to be largely suppressed. The recorded BER performance is shown in Fig. 4. It could be seen that for channel one (1548 nm), the BER performance was improved by 4 dB. For the other channel (1553 nm), an error floor was observed at about $BER=10^{-7}$ in the case of direct amplification while error free operation, with a receiver sensitivity of about -16.5 dB at $BER=10^{-9}$, was achieved for the proposed scheme. The discrepancy in the BER performance for the two different channels was possibly caused

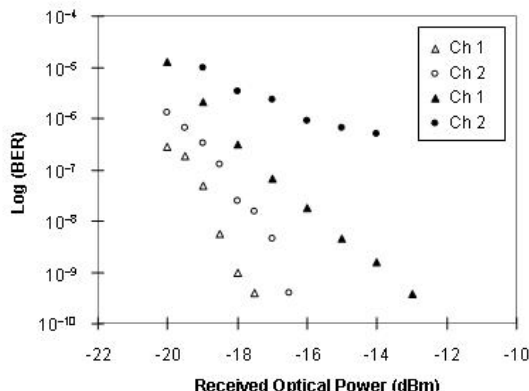


Figure 4 Bit error rate (BER) measurement for two channel inputs of 10-Gb/s PBRS with lengths of 2^7-1 . open symbols: proposed scheme; solid symbols: direct SOA amplification.

by the unequal gain response experienced by each individual wavelength at the SOA.

4. SUMMARY

A simple and effective approach for waveform restoration in SOA gate was proposed and demonstrated. The scheme was based on nonlinear polarization rotation in SOA together with polarimetric filtering. By placing the SOA in a polarization diversified fiber loop configuration, significant improvement in waveform was achieved and the performance was shown to be insensitive to the input signal polarization. Experimental results showed that the input power dynamic range of SOA was extended by over 8 dB. The proposed scheme was also proved to be effective in reducing the XGM-induced channel crosstalk in the SOA with two input wavelength channels.

5. REFERENCES

1. L. F. Tiemeijer, P. J. A. Thijs, et al., *IEEE Photon. Technol. Lett.*, Vol. 7, pp. 284-286, 1995.
2. J. Yu and P. Jeppesen, *J. Lightwave Technol.*, Vol 19, pp. 1316-1326, 2001.
3. K. P. Ho, S. K. Liaw and C. Lin, *Electron. Lett.*, Vol. 32, pp. 2210-2211, 1996.
4. J. Yu and P. Jeppesen, *J. Lightwave Technol.*, vol 19, pp.614-623, 2001.
5. Y. Dong, W. Cai, et al. *Electron. Lett.*, Vol 37, pp 704-705, 2001.

MF99

5:30 PM

Packet-Over-WDM Demonstration and Performance Evaluation of Baseband Optical Carrier-Sense Multiple Access

E. Wong, *University of Melbourne, Melbourne, Australia*; M. Summerfield, *VPIsystems, Melbourne, Australia*, Email: e.wong@ee.mu.oz.au.

We present the first WDM demonstration of baseband optical carrier-sense multiple access with collision avoidance. We evaluate the performance of the node through experiment and theory, showing excellent crosstalk performance and minimal power levels (< -50 dBm) for reliable operation.

1. Introduction

Carrier-sense multiple access with collision avoidance (CSMA/CA) has been proposed as an efficient media access scheme in optical wavelength-routed packet networks [1]-[2]. Each network node uses an optical carrier-sensing capability to prevent transmissions during times when collisions with upstream packets would occur. In earlier work, the sensing of RF subcarriers was implemented for this purpose [1]-[2]. To perform the same function without additional signaling, thus simplifying node design, we proposed in [3] to directly detect the baseband optical signals in the network, and demonstrated the feasibility of this technique in a single channel experiment. In this work, we validate base-

band carrier-sensing for WDM applications. We present the first WDM demonstration of baseband optical CSMA/CA, and assess the sensitivity and crosstalk performance of a node with full add/drop functionality.

Fig. 1 shows a general node architecture that may be employed in baseband optical CSMA/CA ring or bus networks. Each node receives packets on a single wavelength but can transmit packets on any wavelength, achieving full network connectivity. The tapped signals are optically demultiplexed into individual wavelengths, which are then detected by baseband carrier-sense circuits (BCSCs) as shown inset. Each low-bandwidth BCSC performs an envelope detection of the optical packet and generates a control signal to a transmitter unit, which inserts packets accordingly to avoid collisions. A key issue in the deployment of the proposed node architecture is the optical crosstalk at the demultiplexer and the fiber Bragg grating (FBG) of the optical add/drop multiplexer (OADM). Leakage of wavelengths into neighboring output ports at the demultiplexer can erroneously trigger adjacent BCSCs. Likewise, leakage of the Bragg wavelength can cause false triggering at a BCSC of a node further downstream. We show in this work that the impact of crosstalk on the performance of the BCSC and the node is negligible. Another important parameter is the amount of tapped power required at the BCSC to reliably detect packets. We describe a new method to calculate the sensitivity

of the BCSC and compare the results with experiment. To our knowledge, this is the first theoretical sensitivity analysis for any optical carrier-sensing technique. Our BCSC requires less than -50 dBm for reliable carrier-sensing, thus demonstrating that our technique is minimally invasive.

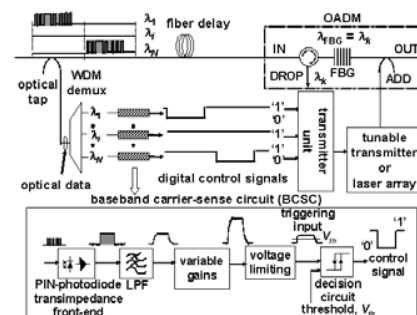


Fig. 1 Baseband optical CSMA/CA node

2. Experiment

Fig. 2 shows the experimental setup used to investigate the performance of a WDM baseband CSMA/CA node. Each Burst Mode Terminal (BMT) comprises a 155 Mb/s burst mode receiver and programmable logic devices, enabling the BMT to be configured as required within the experiment. Each Transmitter Module (TX) is a directly modulated DFB laser. At the upstream section, BMT1 generates randomly spaced 155 Mb/s packets, each comprising a 3-byte header followed by a 128-byte payload ($2^{10} - 1$ PRBS) as shown inset. BMT1 modulates TX1 and TX2 on λ_1 (1532.15 nm) and λ_2 (1532.95 nm) respectively. To provide a constant source of crosstalk at the CSMA/CA node, an unmodulated laser transmits λ_3 (1533.75 nm) in CW mode. The optical signals are combined and launched with equal power (as shown inset by Spectrum S) into a single mode fiber.

At the CSMA/CA node, packets on λ_1 are reflected at the FBG* and received at the DROP port of the OADM, while packets on λ_2 propagate through with λ_3 . To facilitate optical CSMA/CA, a 5/95 optical splitter taps off 5% of the optical power of all upstream signals. An optical attenuator, ATTN, varies the optical power for sensitivity measurements while AWG1, a commercially available standard arrayed waveguide grating (AWG) with 100 GHz spacing, demultiplexes λ_1 and λ_2 for detection at BCSC1 and BCSC2 respectively. When a sufficiently large gap on λ_1 (λ_2) is detected,

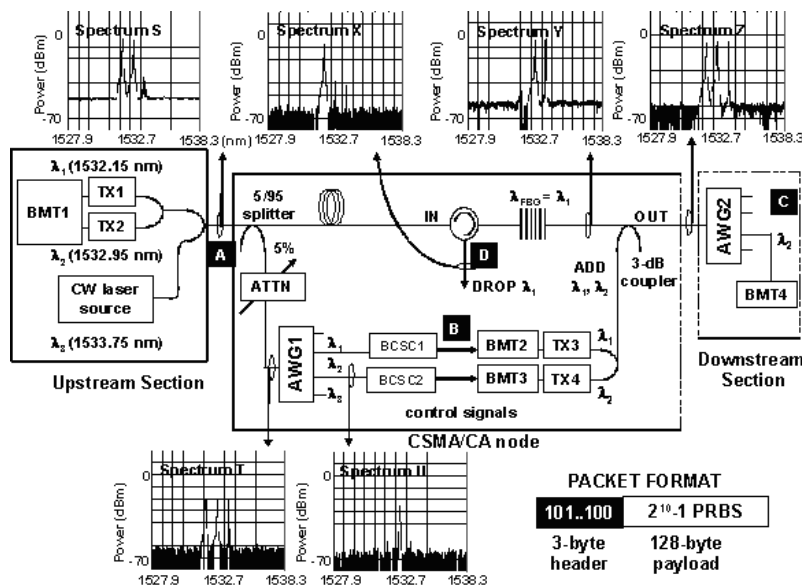


Fig. 2 Experimental setup. BMT: Burst Mode Terminal, TX: Transmitter Module; BCSC: Baseband Carrier-sense Circuit